

Hybrid Au-Si microspheres produced by laser ablation in liquid (LAL) for temperature-feedback, optical nanosensing and anti-counterfeit labeling

V.A. Puzikov^{*1}, S.O. Gurbatov^{1,2}, A.A. Kuchmizhak^{1,2}

¹ Institute of Automation and Control Processes, Far Eastern Branch, Russian Academy of Sciences, Vladivostok 690041, Russia

² Far Eastern Federal University, Vladivostok 690090, Russia

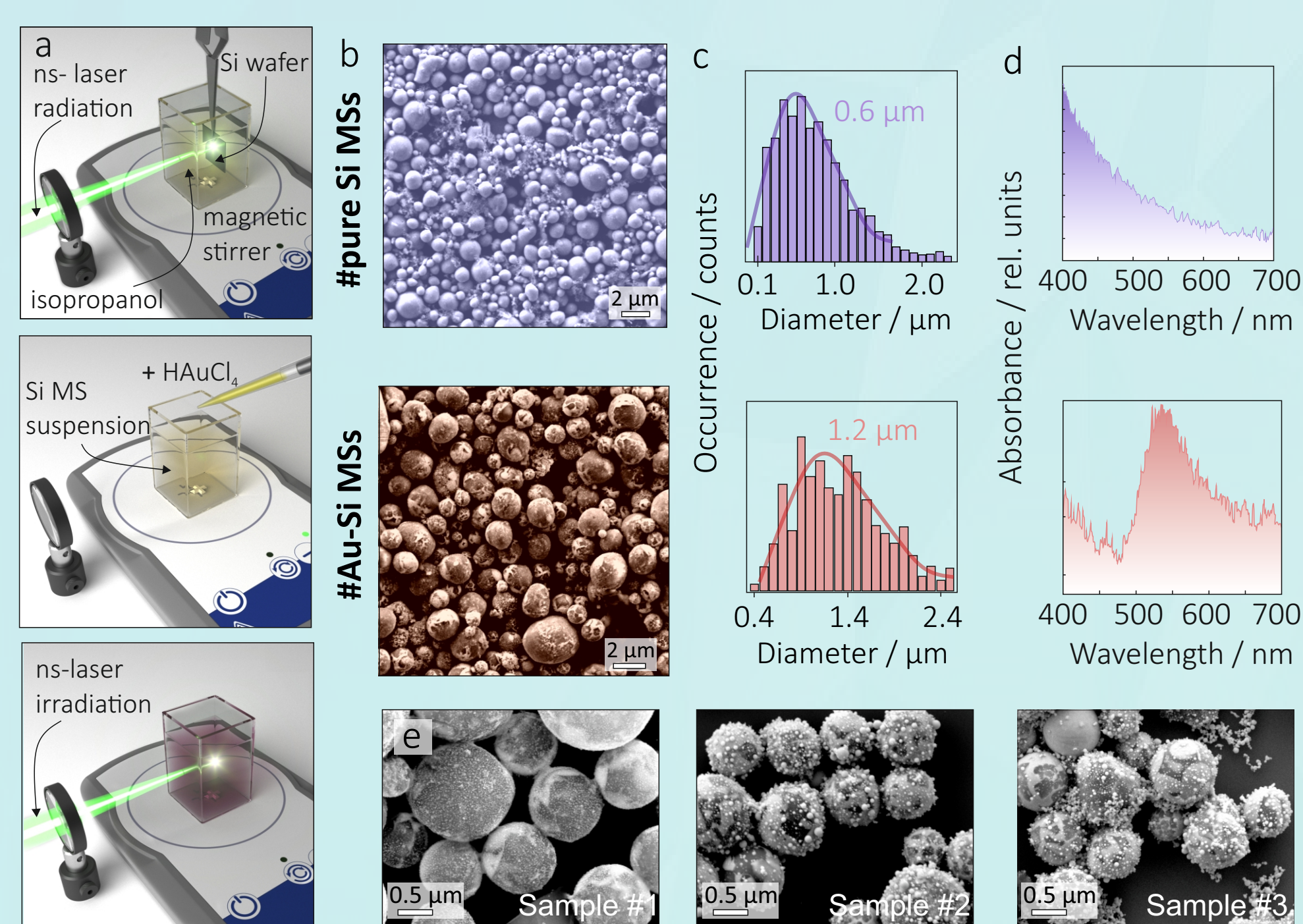


Introduction

Here, we report hybrid Au-Si microspheres (MSs) were produced via ablation of Si wafer by nanosecond (ns)-pulsed laser in isopropanol followed by further irradiation of the as-produced Si dispersion in presence of HAuCl₄. Formation of Au nanoparticles on the surface of Si particles through the thermal reduction of [AuCl₄]⁻ species, as well as further mixing of the metal and semiconductor phases upon remelting and recrystallization, were found to result in a novel hybrid Au-Si product. By combining transmission electron microscopy (TEM), electron tomography, energy-dispersive X-ray spectroscopy (EDX) elemental analysis, X-ray diffraction (XRD) and Raman spectroscopy, we revealed the unique structure of the newly prepared hybrids, in which nanocrystalline Si inclusions are wrapped and decorated with nanostructured Au. Strong light absorbing properties, characteristic Raman signal and nonlinear hot-electron-induced photoluminescence coexisting in the novel Au-Si MSs were proved to be useful for realization of singleparticle SERS sensors with temperature-feedback modality and fabrication of unclonable anti-counterfeit labels.

Fabrication

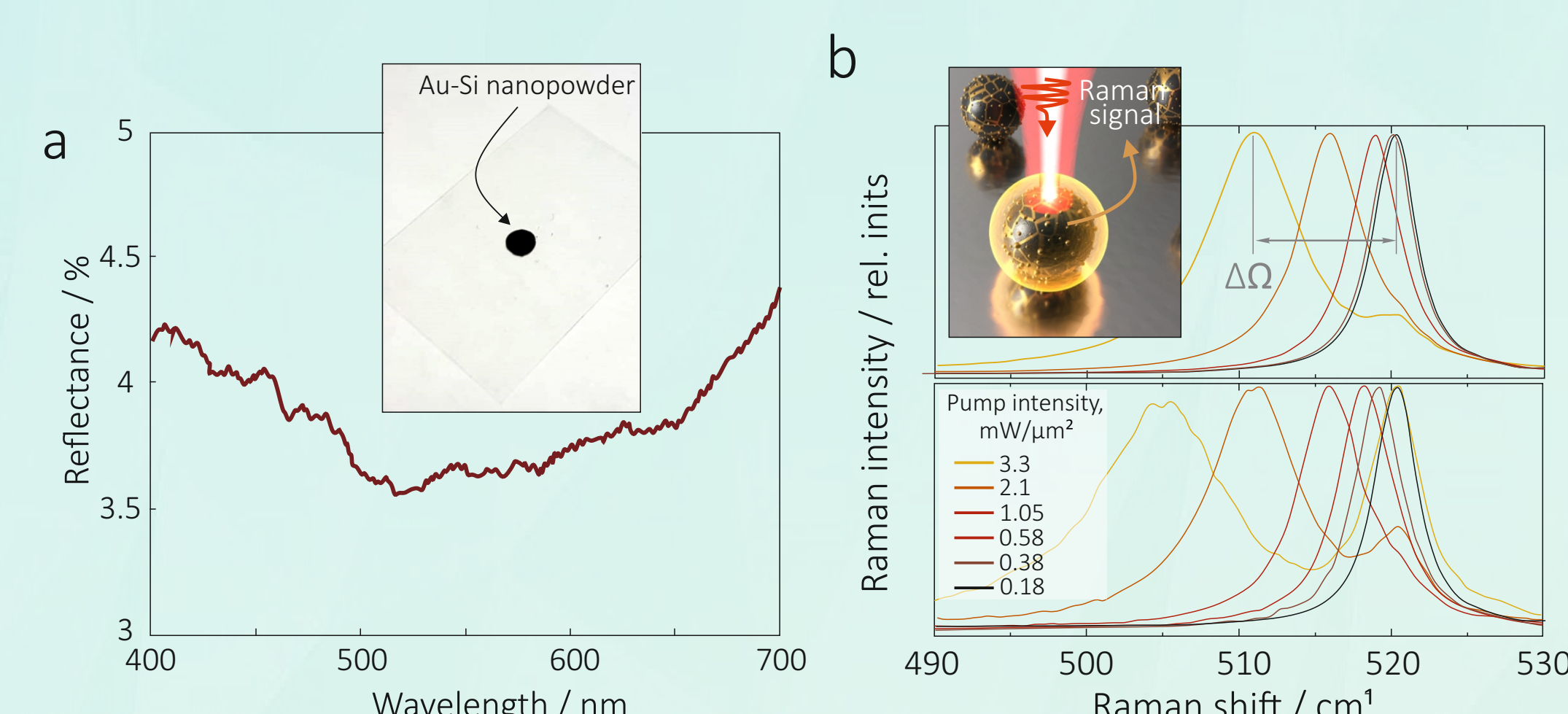
Briefly, a dispersion with Si MSs with an average diameter of $\approx 0.6 \mu\text{m}$ was first produced by ablating a bulk monocrystalline Si wafer immersed in isopropanol (Figure 1b). Next, a certain amount of aqueous HAuCl₄ (10–3M) was added to the as-produced dispersion with Si MSs followed by its laserirradiation for an additional 1 h using the same LAL parameters (pulse energy of 0.4 mJ and pulse repetition rate of 20 Hz). The resultant Au-Si product obtained after adding 0.5 mL of HAuCl₄ solution is shown in the SEM image (Figure 1b) revealing the average particle diameter of $\approx 1.2 \mu\text{m}$. Comparative UV-vis absorbance spectra of the dispersions containing the initial Si precursor and the Au-Si product are presented in Figure 1c.



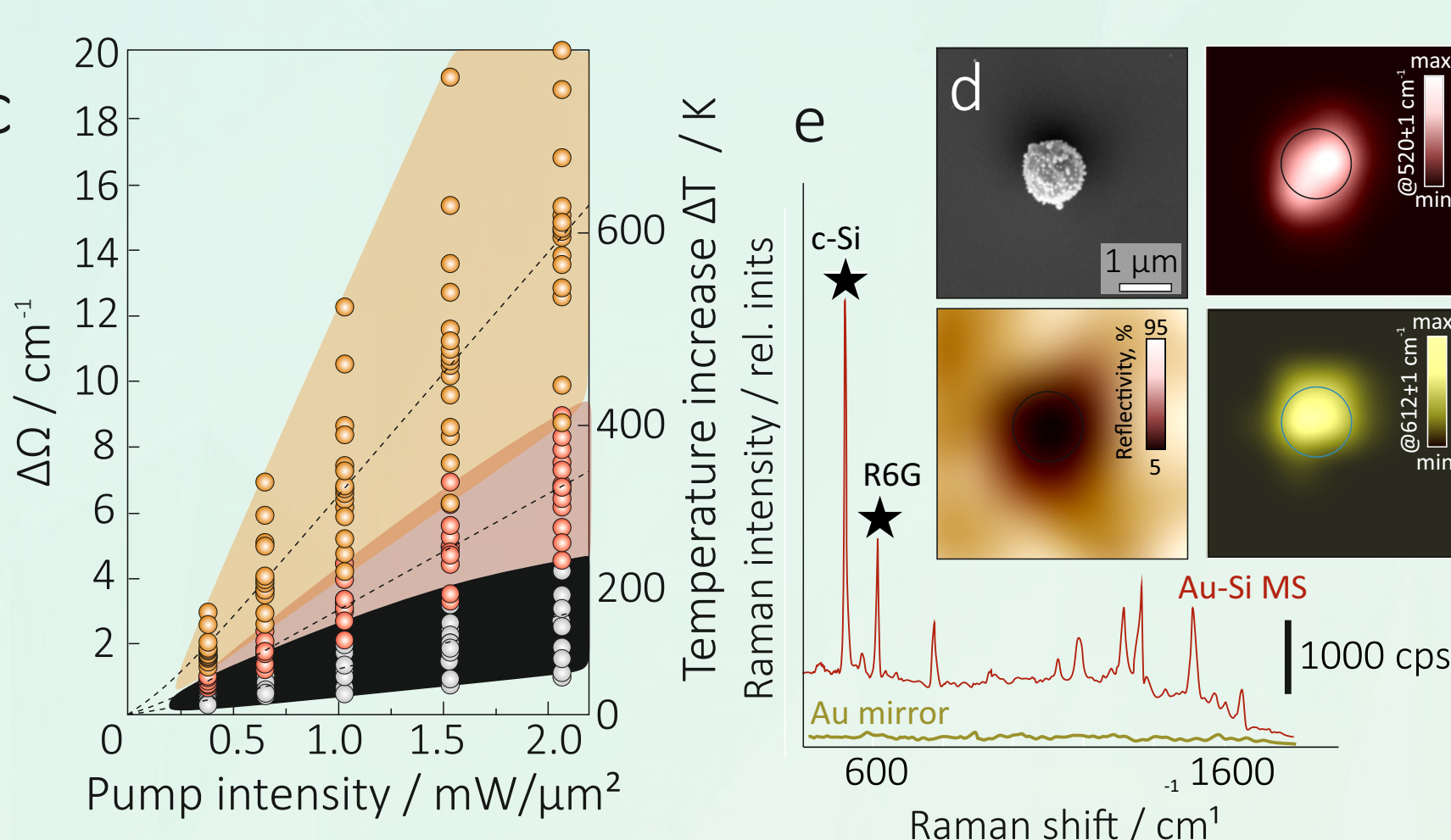
Fabrication of Au-Si MSs. (a) Schematic presentation of preparation of Au-Si hybrid structures via LAL. (b) Representative top-view SEM images, (c) size distributions and (d) normalized UV–vis absorbance spectra (isopropanol suspensions) of Si precursor (top row) and hybrid Au-Si MSs (bottom row, Sample #2). (e) SEM images of Au-Si MSs produced by varying the amount of HAuCl₄ (0.25, 0.5 and 0.75 mM) added to laser-treated suspension.

Light-to-heat conversion

Reflection spectra of the prepared Au-Si powder (Sample #2) drop-cast on a glass slide indicates its average reflectivity $\approx 4\%$ in the visible spectral range with the minimal value ($\approx 3.5\%$) achieved near the plasmonic absorption band of Au constituents (Figure 3(a,b)). Two representative series of Raman spectra measured at different laser pump intensities from isolated MSs randomly chosen from Samples #1 and #3 (top and bottom plots in Figure 3b) demonstrate the remarkably different efficiency of their laserinduced heating. Systematic studies performed for multiple isolated Au-Si MSs produced at varied HAuCl₄ content in the processed dispersion (Samples #1–#3) confirm the direct relationship between Au content and light-to-heat conversion efficiency (Figure 3c). Figure 3d provides correlated SEM, laser confocal and SERS image of a single $1.1\text{-}\mu\text{m}$ -sized Au-Si MS confirming its ability to detect adsorbed analyte molecules at pump intensity ($\approx 0.3 \text{ mW}/\mu\text{m}^2$) while preserving the sensor temperature below that of the analyte's thermal decomposition.



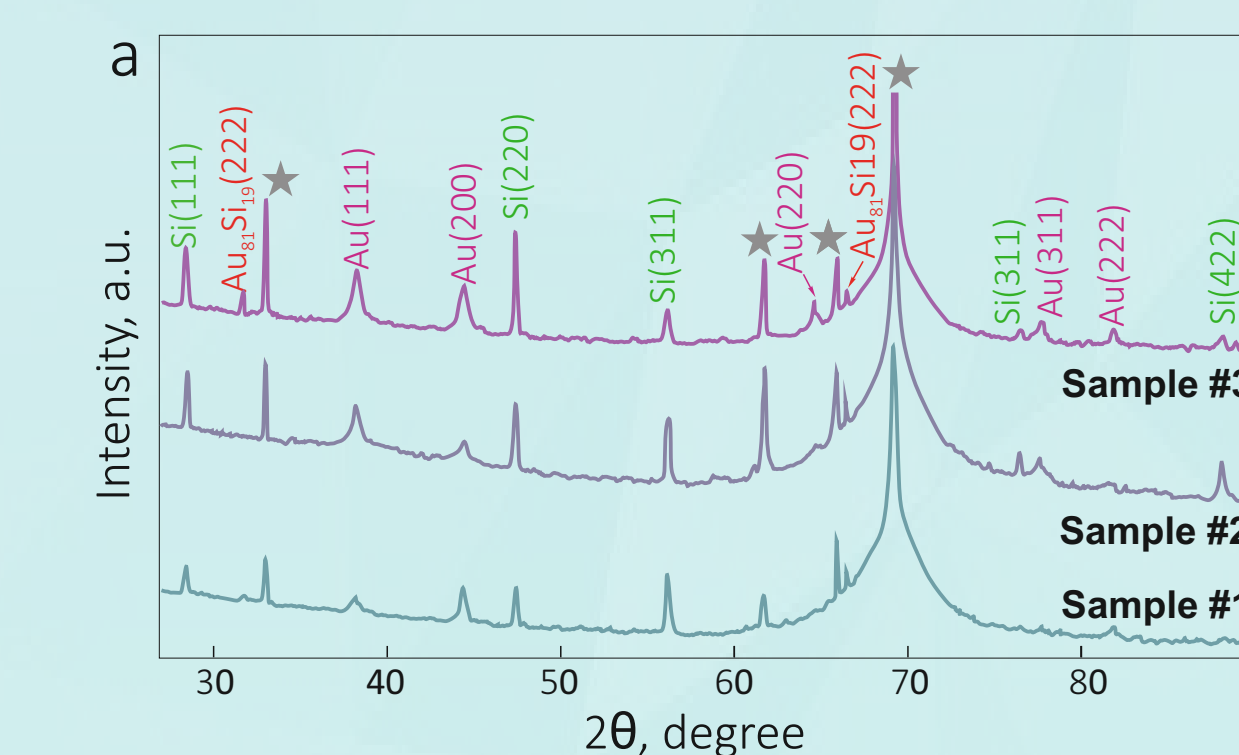
Light-to-heat conversion and single-particle SERS sensing with Au-Si hybrids. (a) Reflectance spectrum of Au-Si MS coating. Inset: Optical photograph of coating made of Au-Si MSs (Sample #2) dried over a glass slide. (b) Representative series of normalized Raman spectra (c-Si band) of separate Au-Si MSs (Samples #2 and #3) measured at varied intensity of pump laser radiation I.



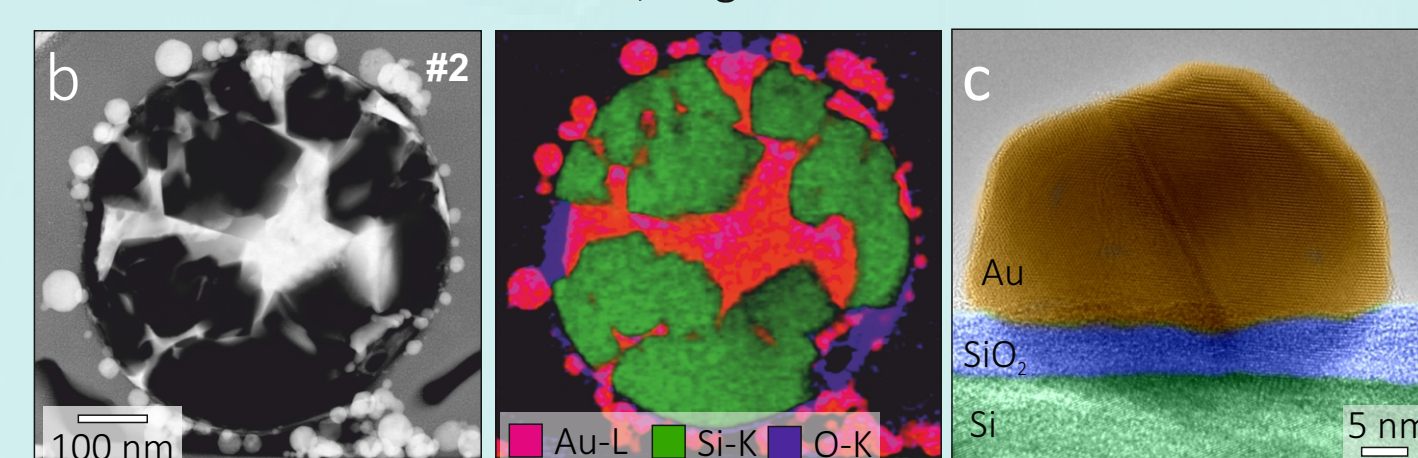
(c) Spectral shift of the c-Si Raman band $\Delta\Omega$ and the average MS temperature increase ΔT versus pump laser intensity I measured for Au-Si MSs from Sample #1 (gray), Sample #2 (red), and Sample #3 (yellow). (d) Correlated SEM, reflection and SERS (at 520.8 ± 1 and $612 \pm 1 \text{ cm}^{-1}$) images of a single Au-Si MS functionalized with R6G molecules. (e) Averaged SERS spectra of the R6G detected from the Au-Si MS and smooth Au mirror sites. Characteristic bands related to crystalline Si and R6G used for mapping are marked by stars. Circle indicates the geometric position of the MS in the optical and Raman images.

Characterization

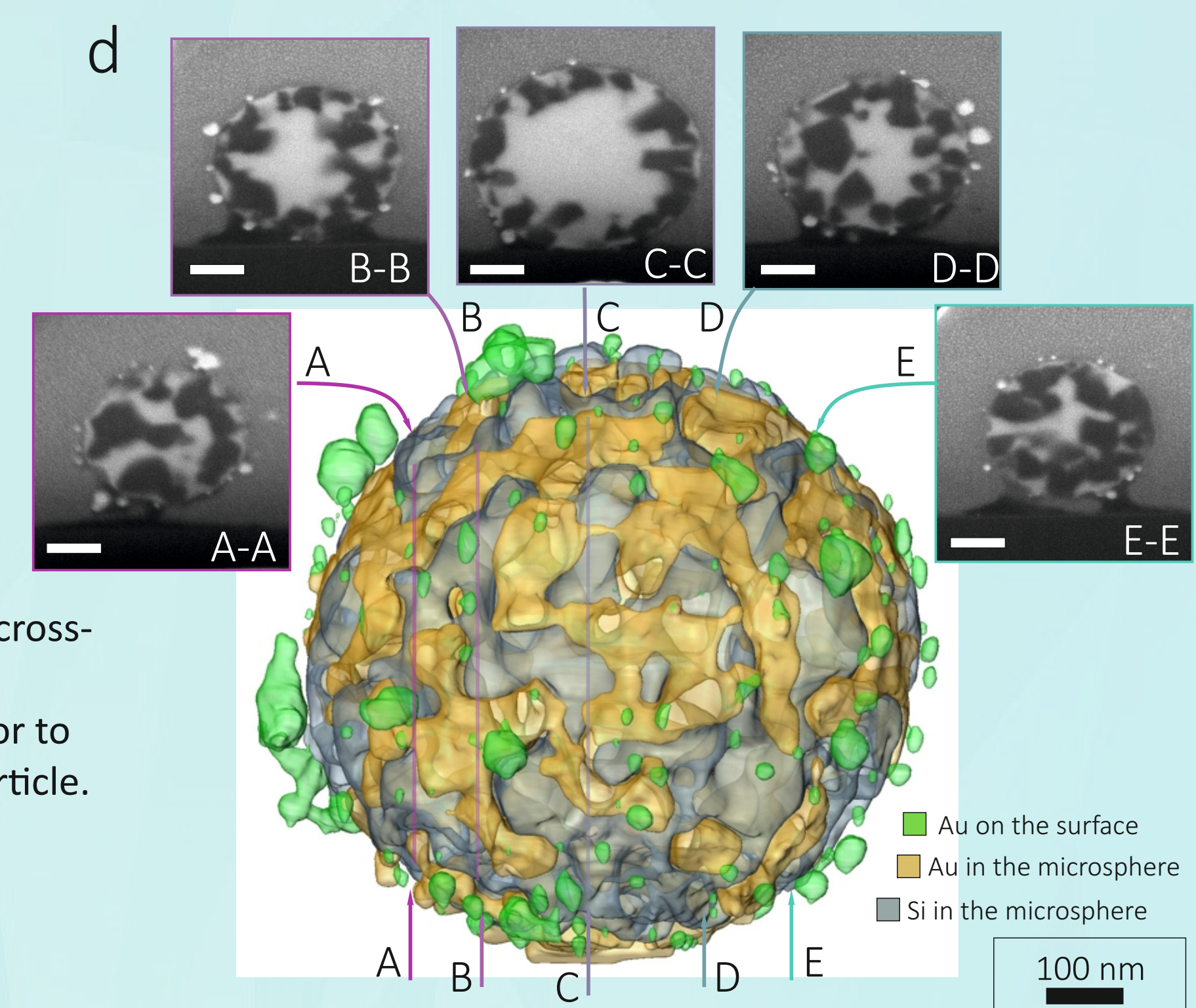
Analysis of SEM images shows that the increase of the amount of HAuCl₄ added to laser-treated mixture results in a visually larger amount of Au (both inside the MSs and on their surface). This finding was confirmed by systematic EDX studies of as-prepared hybrid MSs. The same Au-Si MSs deposited on Si(001) substrate (Samples #1–#3) were further systematically analyzed by XRD revealing several key features regarding the composition and crystal structure of the LAL-prepared hybrids. High-resolution TEM (HR-TEM) was carried out further to study the inner structure and composition of the Au-Si MSs (Samples #1 and #3). Focused ion beam (FIB) milling procedure was undertaken for isolated MSs to prepare their nm-thick lamellae whose representative HR-TEM image is provided in Figure 2b along with superimposed EDX elemental maps. To study the inner structure of the Au-Si hybrids more systematically, a series of consecutive FIB cuts of an isolated MS was prepared, while its 3D model was then reconstructed from a series of corresponding SEM images (Figure 2d).



Characterization of Au-Si MSs. (a) XRD patterns of Au-Si MSs produced at different concentrations of HAuCl₄ added to laser-processed dispersion (Samples #1–#3). Stars denote XRD peaks attributed to the Si substrate used. (b) TEM image and EDX composition mapping of a representative Au-Si MS (Sample #2). (c) HR-TEM image of an isolated Au-Si MS, with a well-seen SiO₂ shell.

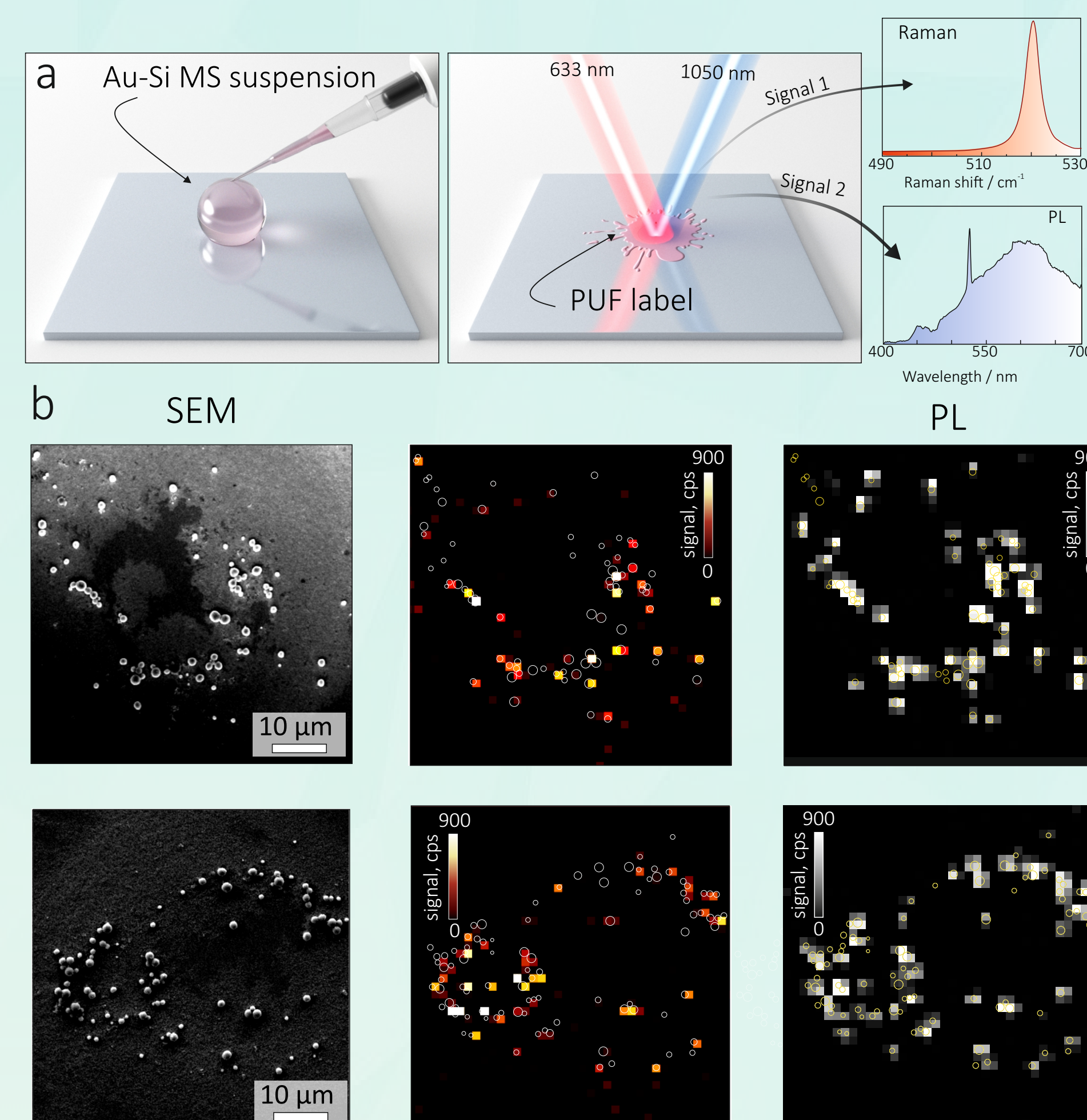


(d) 3D model of an isolated Au-Si MS reconstructed from a series of 50 cross-sectional FIB cuts. Several representative cuts are shown as insets. Au nanoparticles on the surface of a Au-Si MS are highlighted by green color to distinguish them from Au material (orange) mixed with Si within the particle.

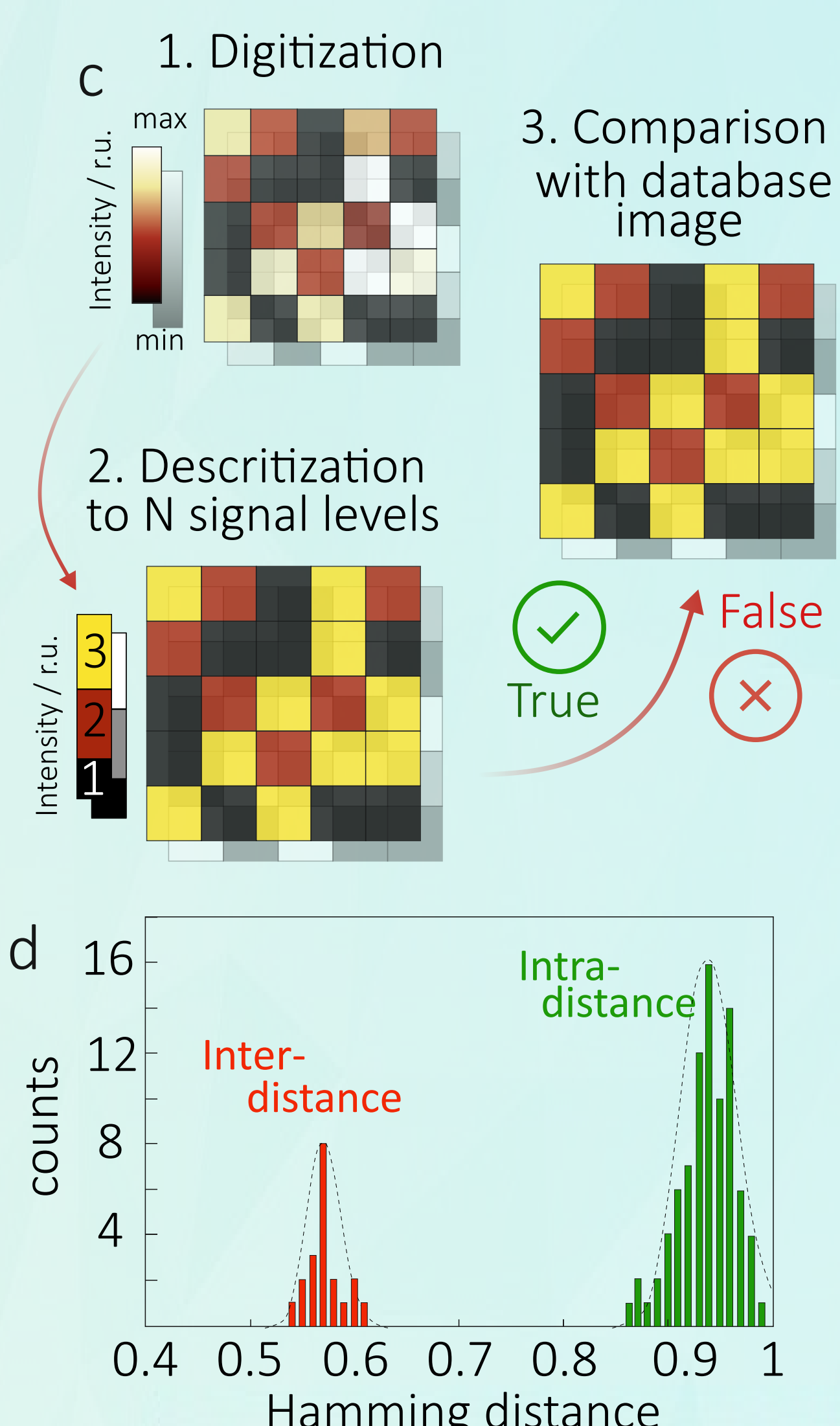


Optical PUF labeling

Here, we produced security tags by drop-casting $0.5\text{-}\mu\text{L}$ drops of as-generated isopropanol dispersion with Au-Si MSs on glass slides or Au mirrors (Figure 4a). Upon drying, the drop-cast material created random arrangements on the surface which are impossible to replicate by chance upon subsequent deposition cycles. Typical examples of Au-Si MS deposits are illustrated by the SEM images in Figure 4b. Figure 4c schematically illustrates the authentication/validation procedure of the produced labels. To justify the ability of the proposed algorithm reliably to distinguish different labels, we characterized 10 random realizations of PUF tags calculating their similarity α (the ratio of zero-intensity pixels to the total pixel number with initial non-zero intensity) or Hamming intra-distance ($1 - \alpha/100\%$). The obtained results are presented in Figure 4d.



Optical PUF labeling with Au-Si hybrids. (a) Schematically illustrated fabrication process of PUF labels and their optical readout by mapping characteristic optical fingerprints: Raman signal and nonlinear broadband photoluminescence associated with crystalline Si inclusions. (b) Correlated SEM, Raman (at 520.8 cm^{-1}) and nonlinear PL images of two representative labels composed of random arrangements of the Au-Si MSs. (c) Sketch of label digitization and authentication. (d) Hamming intra- and inter-distances estimated for 10 different PUF labels.



(c) Sketch of label digitization and authentication. (d) Hamming intra- and inter-distances estimated for 10 different PUF labels.